

Sparse Network Modeling

Moo K. Chung

University of Wisconsin-Madison, USA

mkchung@wisc.edu

July 29, 2020

There have been many attempts to identify high-dimensional network features via multivariate approaches (Chung et al. 2013, Lerch et al. 2006, He et al. 2007, Worsley, Charil, Lerch & Evans 2005, He et al. 2008). Specifically, when the number of voxels or nodes, denoted as p , are substantially larger than the number of images, denoted as n , it produces an under-determined model with infinitely many possible solutions. The *small- n large- p problem* is often remedied by regularizing the under-determined system with additional sparse penalties.

Popular sparse network models include sparse correlations (Lee, Lee, Kang, Kim & Chung 2011, Chung et al. 2013, 2015, 2017), LASSO (Bickel & Levina 2008, Peng et al. 2009, Huang et al. 2009, Chung et al. 2013), sparse canonical correlations (Avants et al. 2010) and graphical-LASSO (Banerjee et al. 2006, 2008, Friedman et al. 2008, Huang et al. 2009, 2010, Mazumder & Hastie 2012, Witten et al. 2011). These popular sparse models require optimizing $L1$ -norm penalties, which has been the major computational bottleneck for solving large-scale problems. Thus, many existing sparse brain network models in brain imaging have been restricted to a few hundreds nodes or less. 2527 MRI features used in a LASSO model for Alzheimer’s disease (Xin et al. 2015) is probably the largest number of features used in any sparse model in the brain imaging literature.

1 Why sparse network models?

If we are interested quantifying the measurements in every voxel in an image simultaneously, the standard procedure is to set up a multivariate general linear model (MGLM), which generalizes widely used univariate GLM by incorporating vector valued responses and explanatory variables (Anderson 1984, Friston et al. 1995, Worsley et al. 1996, 2004, Taylor & Worsley 2008, Chung et al. 2010). Hotelling’s T^2 -statistic is a special case of MGLM and has been mainly used for inference on surface shapes and deformations (Thompson et al. 1997, Joshi 1998, Cao & Worsley 1999, Gaser et al. 1999, Chung et al. 2001).

Let $\mathbf{J}_{n \times p} = (J_{ij})$ be the measurement matrix, J_{ij} is the measurement for subject i at voxel position j . The subscripts denote the dimension of matrix. We can think J_{ij} as either Jacobian determinant, fractional anisotropy values or fMRI activation. Assume there are total n subjects and p voxels of interest. The

measurement vector at the j -th voxel is denoted as $\mathbf{x}_j = (J_{1j}, \dots, J_{nj})^\top$. The measurement vector for the i -th subject is denoted as $\mathbf{y}_i = (J_{i1}, \dots, J_{ip})$, which is expected to be distributed identically and independently over subjects. Note that

$$\mathbf{J} = (\mathbf{x}_1, \dots, \mathbf{x}_p) = (\mathbf{y}_1^\top, \dots, \mathbf{y}_n^\top)^\top.$$

We may assume the covariance matrix of \mathbf{y}_i to be

$$\mathbb{V}(\mathbf{y}_1) = \dots = \mathbb{V}(\mathbf{y}_n) = \boldsymbol{\Sigma}_{p \times p} = (\sigma_{kl}).$$

With these notations, we set up the following MGLM over all subjects and across different voxel positions:

$$\mathbf{J}_{n \times p} = \mathbf{X}_{n \times k} \mathbf{B}_{k \times p} + \mathbf{Z}_{n \times q} \mathbf{G}_{q \times p} + \mathbf{U}_{n \times p} \boldsymbol{\Sigma}_{p \times p}^{1/2}, \quad (1)$$

where \mathbf{X} is the matrix of contrasted explanatory variables while \mathbf{B} is the matrix of unknown coefficients to be estimated. Nuisance covariates of non-interest are in the matrix \mathbf{Z} and the corresponding coefficients are in the matrix \mathbf{G} . The components of Gaussian random matrix \mathbf{U} are independently distributed with zero mean and unit variance. The symmetric matrix $\boldsymbol{\Sigma}^{1/2}$ is the square-root of the covariance matrix accounting for the spatial dependency across different voxels. In MGLM (1), we are interested in testing the null hypothesis

$$H_0 : \mathbf{B} = \mathbf{0}.$$

The parameter matrices in the model are estimated via the least squares method. The resulting multivariate test statistics are called the Lawley-Hotelling trace or Roy's maximum root. When there is only one voxel, i.e. $p = 1$, these multivariate test statistics collapses to Hotelling's T^2 -statistic (Worsley et al. 2004).

Note that MGLM (1) is equivalent to the assumption that \mathbf{y}_i follows multivariate normal with some mean μ and covariance $\boldsymbol{\Sigma}$, i.e., $\mathbf{y}_i \sim N(\mu, \boldsymbol{\Sigma})$. Then neglecting constant terms, the log-likelihood function L of \mathbf{y}_i is given by

$$L(\mu, \boldsymbol{\Sigma}) = \log \det \boldsymbol{\Sigma}^{-1} - \frac{1}{n} \sum_{i=1}^n (\mathbf{y}_i - \mu)^\top \boldsymbol{\Sigma}^{-1} (\mathbf{y}_i - \mu).$$

By maximizing the log-likelihood, MLE of μ and $\boldsymbol{\Sigma}$ are given by

$$\begin{aligned} \hat{\mu} &= \bar{\mathbf{y}}_i = \frac{1}{n} \sum_{i=1}^n \mathbf{y}_i \\ \hat{\boldsymbol{\Sigma}} &= \frac{1}{n} \sum_{i=1}^n (\mathbf{y}_i - \bar{\mathbf{y}}_i)^\top (\mathbf{y}_i - \bar{\mathbf{y}}_i). \end{aligned} \quad (2)$$

For a notational convenience, we can center the measurement \mathbf{y}_i such that

$$\mathbf{y}_i \leftarrow \mathbf{y}_i - \bar{\mathbf{y}}_i.$$

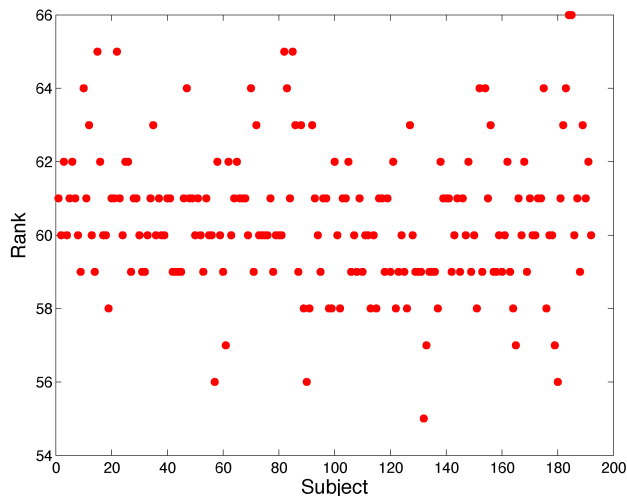


Fig. 1: The rank of 80-nodes fMRI correlation matrices for 192 subjects published in (Qiu et al. 2015). None of correlation matrix is of full rank and not invertible. Many brain regions show pairwise correlations.

We are basically centering the measurements by subtracting the group mean over subjects. Then MLE (3) can be written in a more compact form

$$\hat{\Sigma} = \frac{1}{n} \mathbf{J}_{p \times n}^{\top} \mathbf{J}_{n \times p}. \quad (3)$$

However, there is a serious defect with MGLM (1) and its MLE (3); namely the estimated covariance matrix $\hat{\Sigma}$ is positive definite only for $n \geq p$ (Friston et al. 1995, Schäfer & Strimmer 2005). $\mathbf{J}^{\top} \mathbf{J}$ becomes rank deficient for $n < p$. In most imaging studies, there are more voxels than the number of subjects, i.e., $n < p$. Even when $n > p$, for various reasons, correlation and covariance matrices may not be full rank (Figure 1). When $\hat{\Sigma}$ is singular, we do not properly have the inverse of $\hat{\Sigma}$, which is the precision matrix often needed in partial correlation based network analyses (Lee, Lee, Kang, Kim & Chung 2011). This is the main reason MGLM was rarely employed over the whole brain region and researchers are still using mostly univariate approaches in imaging studies.

1.1 Why sparse network?

The majority of functional and structural connectivity studies in brain imaging are usually performed following the standard analysis framework (Gong et al. 2009, Hagmann et al. 2007, Fornito et al. 2010, Zalesky et al. 2010). From 3D whole brain images, n regions of interest (ROI) are identified and serve as the nodes of the brain network. Measurements at ROIs are then correlated in a pairwise fashion to produce the connectivity matrix of size $n \times n$. The connectivity

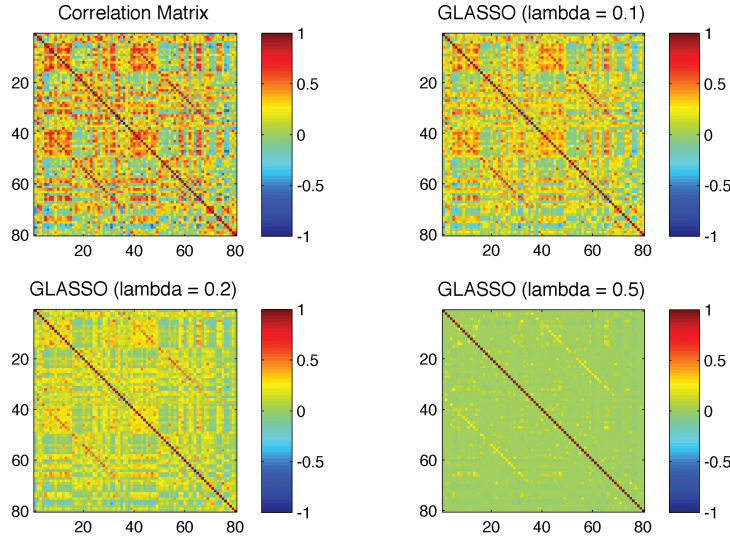


Fig. 2: Graphical-LASSO estimation on an original singular correlation matrix from study Qiu et al. (2015). The original correlation matrix has the rank of 61 indicating approximately 19 nodes out of 80 nodes are dependent of other nodes. As the sparse parameter λ increases, we see more sparsity and diagonal dominance that makes the estimated sparse correlation matrix to be more positive definite.

matrix is then thresholded to produce the adjacency matrix consisting of zeros and ones that define the link between two nodes. The binarized adjacency matrix is then used to construct the brain network. Then various graph complexity measures such as degree, clustering coefficients, entropy, path length, hub centrality and modularity are defined on the graph and the subsequent statistical inference is performed on these complexity measures.

For a large number of nodes, simple thresholding of correlation will produce a large number of edges which makes the interpretation difficult. For example, for 3×10^5 voxels in an image, we can possibly have a total of 9×10^{10} directed edges in the graph. For this reason we used the sparse data recovery framework in obtaining a far smaller number of significant edges.

2 Sparse likelihood

Beyond sparse regression, others have proposed the likelihood methods. To remedy the small- n and large- p problem, the likelihood is regularized with a L1-norm penalty. If we center the measurements \mathbf{y}_i , the log-likelihood can be written

as

$$\begin{aligned} L(\boldsymbol{\Sigma}) &= \log \det \boldsymbol{\Sigma}^{-1} - \frac{1}{n} \sum_{i=1}^n \mathbf{y}_i^\top \boldsymbol{\Sigma}^{-1} \mathbf{y}_i \\ &= \log \det \boldsymbol{\Sigma}^{-1} - \text{tr}(\boldsymbol{\Sigma}^{-1} S), \end{aligned}$$

where $S = \frac{1}{n} \sum_{i=1}^n \mathbf{y}_i^\top \mathbf{y}_i$ is the sample covariance matrix. We used the fact that the trace of a scalar value is equivalent to the scalar value itself and $\text{tr}(AB) = \text{tr}(BA)$ for matrices A and B .

To avoid the small- n large- p problem, we penalize the log-likelihood with L1-norm penalty:

$$L(\boldsymbol{\Sigma}^{-1}) = \log \det \boldsymbol{\Sigma}^{-1} - \text{tr}(\boldsymbol{\Sigma}^{-1} S) - \lambda \|\boldsymbol{\Sigma}^{-1}\|_1, \quad (4)$$

where $\|\cdot\|_1$ is the sum of the absolute values of the elements. We made the likelihood as a function of $\boldsymbol{\Sigma}^{-1}$ to simply emphasize that we are trying to estimate the inverse covariance matrix. The penalized log-likelihood is maximized over the space of all possible symmetric positive definite matrices. (4) is a convex problem and it is usually solved using the graphical-LASSO (GLASSO) algorithm (Banerjee et al. 2006, 2008, Friedman et al. 2008, Huang et al. 2010, Mazumder & Hastie 2012). The tuning parameter $\lambda > 0$ controls the sparsity of the off-diagonal elements of the inverse covariance matrix. By increasing $\lambda > 0$, the estimated inverse covariance matrix becomes more sparse (Figure 2).

GLASSO is a fairly time consuming algorithm (Friedman et al. 2008, Huang et al. 2010). Solving GLASSO for 548 nodes, for instance, may take up to 6 minutes on slow desktop computers if fast algorithms like Hsieh et al. (2013) is not used. If $\boldsymbol{\Sigma}_i^{-1}(\lambda)$ is the estimated inverse sparse covariance for group i at given sparse parameter λ , we are interested in testing the equivalence of inverse covariance matrices between the two groups at fixed λ , i.e.,

$$H_0 : \boldsymbol{\Sigma}_1^{-1}(\lambda) = \boldsymbol{\Sigma}_2^{-1}(\lambda).$$

2.1 Filtration in graphical-LASSO

The solution to graphical-LASSO has a peculiar nested topological structure. Let $\boldsymbol{\Sigma}^{-1}(\lambda) = (\sigma^{ij}(\lambda))$ be the inverse covariance estimated from graphical-LASSO. Let $A(\lambda) = (a_{ij})$ be the corresponding adjacency matrix given by

$$a_{ij}(\lambda) = \begin{cases} 1 & \text{if } \hat{\sigma}^{ij} \neq 0; \\ 0 & \text{otherwise.} \end{cases} \quad (5)$$

The adjacency matrix A induces a graph $\mathcal{G}(\lambda)$ consisting of $\kappa(\lambda)$ number of partitioned subgraphs

$$\mathcal{G}(\lambda) = \bigcup_{l=1}^{\kappa(\lambda)} G_l(\lambda) \quad \text{with } G_l = \{V_l(\lambda), A_l(\lambda)\},$$

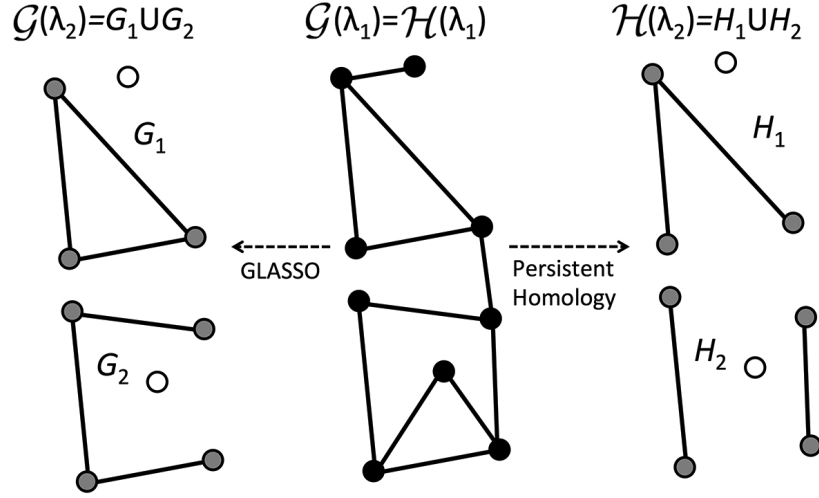


Fig. 3: Schematic of graph filtrations obtained by sparse-likelihood (5) and sample covariance thresholding (6). The vertex set of $\mathcal{G}(\lambda_1) = \mathcal{H}(\lambda_1)$ consists of black nodes. For the next filtration value λ_2 , $\mathcal{G}(\lambda_2) \neq \mathcal{H}(\lambda_2)$ since the edge sets are different. However, the partitioned vertex sets (gray colored) of $\mathcal{G}(\lambda_2)$ and $\mathcal{H}(\lambda_2)$ match.

where V_l and A_l are node and edge sets of subgraph G_l .

Let $S = (s_{ij})$ be the sample covariance matrix. Let $B(\lambda) = (b_{ij})$ be the adjacency matrix defined by

$$b_{ij}(\lambda) = \begin{cases} 1 & \text{if } |\widehat{s}_{ij}| > \lambda; \\ 0 & \text{otherwise.} \end{cases} \quad (6)$$

The adjacency matrix B similarly induces a graph with $\tau(\lambda)$ disjoint subgraphs:

$$\mathcal{H}(\lambda) = \bigcup_{l=1}^{\tau(\lambda)} H_l(\lambda) \quad \text{with } H_l = \{W_l(\lambda), B_l(\lambda)\},$$

where W_l and B_l are node and edge sets of subgraph H_l . Then the partitioned graphs are shown to be partially nested in a sense that the node sets exhibits persistency.

Theorem 1. *For any $\lambda > 0$, the adjacency matrices (5) and (6) induce the identical vertex partition so that $\kappa(\lambda) = \tau(\lambda)$ and $V_l(\lambda) = W_l(\lambda)$. Further, the node sets V_l and W_l form filtrations over the sparse parameter:*

$$V_l(\lambda_1) \supset V_l(\lambda_2) \supset V_l(\lambda_3) \supset \cdots \quad (7)$$

$$W_l(\lambda_1) \supset W_l(\lambda_2) \supset W_l(\lambda_3) \supset \cdots \quad (8)$$

for $\lambda_1 \leq \lambda_2 \leq \lambda_3 \leq \cdots$.

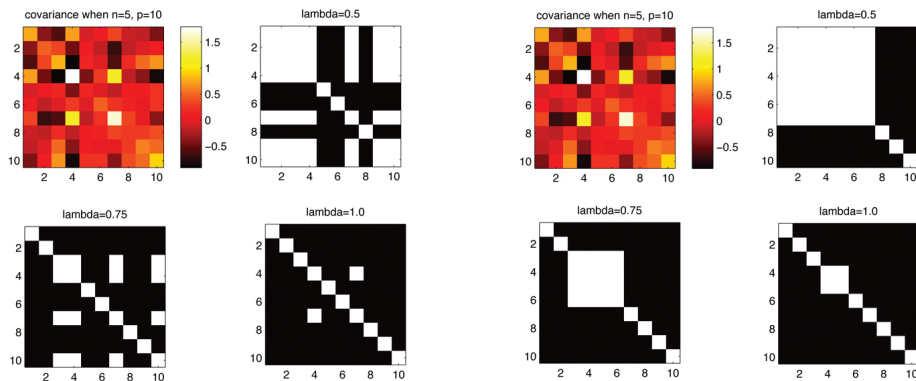


Fig. 4: Left: Adjacency matrices obtained through graphical-LASSO with increasing λ values. The persistent homological structure is self-evident. Right: Adjacency matrices are clustered as a block diagonal matrix D by permutation.

From (6), it is trivial to see the filtration holds for W_l . The filtration for V_l is proved in Huang et al. (2010). The equivalence of the node sets $V_l = W_l$ is proved in Mazumder & Hastie (2012). Note that the edge sets may not form a filtration (Figure 3). The construction of the filtration on the node sets V_l (7) is very time consuming since we have to solve the sequence of graphical-LASSO. For instance, for 548 node sets and 547 different filtration values, the whole filtration takes more than 54 hours in a desktop (Chung et al. 2015).

In Figure 4, we randomly simulated the data matrix $X_{5 \times 10}$ from the standard normal distribution. The sample covariance matrix is then feed into graphical-LASSO with different filtration values. To identify the structure better, we transformed the adjacency matrix A by permutation P such that $D = PAP^{-1}$ is a block diagonal matrix. Theoretically only the partitioned node sets are expected to exhibit the nestedness but in this example, the edge sets are also nested as well.

3 Sparse correlation network

The problem with graphical-LASSO or any type of similar L1 norm optimization is that it becomes computationally expensive as the number of node p increases. So it is not really practical for large-scale brain networks. In this section, we present a scalable large-scale network model ($p > 25000$) that yields greater computational speed and efficiency by bypassing the computational bottleneck of optimizing L1-penalties.

There are few previous studies at speeding up the computation for sparse models. By identifying block diagonal structures in the estimated (inverse) covariance matrix, it is possible to reduce the computational burden in the penalized log-likelihood method (Mazumder & Hastie 2012, Witten et al. 2011).

However, the method presented in this section differs from Mazumder & Hastie (2012) and Witten et al. (2011) in that we do not need to assume that the data to follow Gaussianity. Subsequently, there is no need to specify the likelihood function. Further, the cost functions we are optimizing are different. Specifically, we propose a novel sparse network model based on *correlations*. Although correlations are often used in sciences in connection to times series and stochastic processes (Worsley, Charil, Lerch & Evans 2005, Worsley, Chen, Lerch & Evans 2005), the sparse version of correlation has been somewhat neglected.

Consider measurement vector \mathbf{x}_j on node j . If we center and rescale the measurement \mathbf{x}_j such that

$$\|\mathbf{x}_j\|^2 = \mathbf{x}_j^\top \mathbf{x}_j = 1,$$

the sample correlation between nodes i and j is given by $\mathbf{x}_i^\top \mathbf{x}_j$. Since the data is normalized, the sample covariance matrix is reduced to the sample correlation matrix.

Consider the following linear regression between nodes j and k ($k \neq j$):

$$\mathbf{x}_j = \gamma_{jk} \mathbf{x}_k + \epsilon_j. \quad (9)$$

We are basically correlating data at node j to data at node k . In this particular case, γ_{jk} is the usual Pearson correlation. The least squares estimation (LSE) of γ_{jk} is then given by

$$\hat{\gamma}_{jk} = \mathbf{x}_j^\top \mathbf{x}_k, \quad (10)$$

which is the sample correlation. For the normalized data, regression coefficient estimation is exactly the sample correlation. For the normalized and centered data, the regression coefficient is the correlation. It can be shown that (22) minimizes the sum of least squares over all nodes:

$$\sum_{j=1}^p \sum_{k \neq j} \|\mathbf{x}_j - \gamma_{jk} \mathbf{x}_k\|^2. \quad (11)$$

Note that we do not really care about correlating \mathbf{x}_j to itself since the correlation is then trivially $\gamma_{jj} = 1$.

3.1 Sparse correlations

Let $\mathbf{\Gamma} = (\gamma_{jk})$ be the correlation matrix. The sparse penalized version of (21) is given by

$$F(\mathbf{\Gamma}) = \frac{1}{2} \sum_{j=1}^p \sum_{k \neq j} \|\mathbf{x}_j - \gamma_{jk} \mathbf{x}_k\|^2 + \lambda \sum_{j=1}^p \sum_{k \neq j} |\gamma_{jk}|. \quad (12)$$

The sparse correlation is given by minimizing $F(\mathbf{\Gamma})$. By increasing λ , the estimated correlation matrix $\hat{\mathbf{\Gamma}}(\lambda)$ becomes more sparse. When $\lambda = 0$, the sparse

correlation is simply given by the sample correlation, i.e. $\hat{\gamma}_{jk} = \mathbf{x}_j^\top \mathbf{x}_k$. As λ increases, the correlation matrix $\mathbf{\Gamma}$ shrinks to zero and becomes more sparse. This is separable compressed sensing or LASSO type problem. However, there is no need to numerically optimize (23) using the coordinate descent learning or the active-set algorithm often used in compressed sensing (Peng et al. 2009, Friedman et al. 2008). The minimization of (23) can be done by the proposed soft-thresholding method analytically by exploiting the topological structure of the problem. Since $\mathbf{x}_i^\top \mathbf{x}_j \neq \delta_{ij}$, the Dirac delta, it looks like the sparse regression is not orthogonal design and the existing soft-thresholding method for LASSO (Tibshirani 1996) is not directly applicable. However, it can be made into orthogonal design. The detail is given in the sparse cross-correlation section.

Theorem 2. For $\lambda \geq 0$, the solution of the following separable LASSO problem

$$\hat{\gamma}_{jk}(\lambda) = \arg \min_{\gamma_{jk}} \frac{1}{2} \sum_{j=1}^p \sum_{k \neq j} \|\mathbf{x}_j - \gamma_{jk} \mathbf{x}_k\|^2 + \lambda \sum_{j=1}^p \sum_{k \neq j} |\gamma_{jk}|,$$

is given by the soft-thresholding

$$\hat{\gamma}_{jk}(\lambda) = \begin{cases} \mathbf{x}_j^\top \mathbf{x}_k - \lambda & \text{if } \mathbf{x}_j^\top \mathbf{x}_k > \lambda \\ 0 & \text{if } |\mathbf{x}_j^\top \mathbf{x}_k| \leq \lambda \\ \mathbf{x}_j^\top \mathbf{x}_k + \lambda & \text{if } \mathbf{x}_j^\top \mathbf{x}_k < -\lambda \end{cases}. \quad (13)$$

Proof. Write (23) as

$$F(\mathbf{\Gamma}) = \frac{1}{2} \sum_{j=1}^p \sum_{k \neq j} f(\gamma_{jk}), \quad (14)$$

where

$$f(\gamma_{jk}) = \|\mathbf{x}_j - \gamma_{jk} \mathbf{x}_k\|^2 + 2\lambda |\gamma_{jk}|.$$

Since $f(\gamma_{jk})$ is nonnegative and convex, $F(\mathbf{\Gamma})$ is minimum if each component $f(\gamma_{jk})$ achieves minimum. So we only need to minimize each component $f(\gamma_{jk})$. This differentiates our sparse correlation formulation from the standard compressed sensing that cannot be optimized in this component wise fashion. $f(\gamma_{jk})$ can be rewritten as

$$\begin{aligned} f(\gamma_{jk}) &= \|\mathbf{x}_j\|^2 - 2\gamma_{jk} \mathbf{x}_j^\top \mathbf{x}_k + \gamma_{jk}^2 \|\mathbf{x}_k\|^2 + 2\lambda |\gamma_{jk}| \\ &= (\gamma_{jk} - \mathbf{x}_j^\top \mathbf{x}_k)^2 + 2\lambda |\gamma_{jk}| + 1. \end{aligned}$$

We used the fact $\mathbf{x}_j^\top \mathbf{x}_j = 1$.

For $\lambda = 0$, the minimum of $f(\gamma_{jk})$ is achieved when $\gamma_{jk} = \mathbf{x}_j^\top \mathbf{x}_k$, which is the usual LSE. For $\lambda > 0$, Since $f(\gamma_{jk})$ is quadratic in γ_{jk} , the minimum is achieved when

$$\frac{\partial f}{\partial \gamma_{jk}} = 2\gamma_{jk} - 2\mathbf{x}_j^\top \mathbf{x}_k \pm 2\lambda = 0 \quad (15)$$

The sign of λ depends on the sign of γ_{jk} . Thus, sparse correlation $\widehat{\gamma}_{jk}$ is given by a soft-thresholding of $\mathbf{x}_j^\top \mathbf{x}_k$:

$$\widehat{\gamma}_{jk}(\lambda) = \begin{cases} \mathbf{x}_j^\top \mathbf{x}_k - \lambda & \text{if } \mathbf{x}_j^\top \mathbf{x}_k > \lambda \\ 0 & \text{if } |\mathbf{x}_j^\top \mathbf{x}_k| \leq \lambda \\ \mathbf{x}_j^\top \mathbf{x}_k + \lambda & \text{if } \mathbf{x}_j^\top \mathbf{x}_k < -\lambda \end{cases} . \quad (16)$$

□

The estimated sparse correlation (16) basically thresholds the sample correlation that is larger or smaller than λ by the amount λ . Due to this simple expression, there is no need to optimize (23) numerically as often done in compressed sensing or LASSO (Peng et al. 2009, Friedman et al. 2008). However, Theorem 2 is only applicable to separable cases and for non-separable cases, numerical optimization is still needed.

The different choices of sparsity parameter λ will produce different solutions in sparse model $\mathcal{A}(\lambda)$. Instead of analyzing each model separately, we can analyze the whole collection of all the sparse solutions for many different values of λ . This avoids the problem of identifying the optimal sparse parameter that may not be optimal in practice. The question is then how to use the collection of $\mathcal{A}(\lambda)$ in a coherent mathematical fashion. This can be addressed using persistent homology (Edelsbrunner & Harer 2008, Lee, Chung, Kang, Kim & Lee 2011, Lee et al. 2012).

3.2 Filtration in sparse correlations

Using the sparse solution (16), we can construct a filtration. We will basically build a graph \mathcal{G} using sparse correlations. Let $\widehat{\gamma}_{jk}(\lambda)$ be the sparse correlation estimate. Let $A(\lambda) = (a_{ij})$ be the adjacency matrix defined as

$$a_{jk}(\lambda) = \begin{cases} 1 & \text{if } \widehat{\gamma}_{jk}(\lambda) \neq 0; \\ 0 & \text{otherwise.} \end{cases}$$

This is equivalent to the adjacency matrix $B = (b_{jk})$ defined as

$$b_{jk}(\lambda) = \begin{cases} 1 & \text{if } |\mathbf{x}_j^\top \mathbf{x}_k| > \lambda; \\ 0 & \text{otherwise.} \end{cases} \quad (17)$$

The adjacency matrix B is simply obtained by thresholding the sample correlations. Then the adjacency matrices A and B induce a identical graph $\mathcal{G}(\lambda)$ consisting of $\kappa(\lambda)$ number of partitioned subgraphs

$$\mathcal{G}(\lambda) = \bigcup_{l=1}^{\kappa(\lambda)} G_l(\lambda) \quad \text{with } G_l = \{V_l(\lambda), E_l(\lambda)\},$$

where V_l and E_l are node and edge sets respectively. Note

$$G_l \cap G_m = \emptyset \quad \text{for any } l \neq m.$$

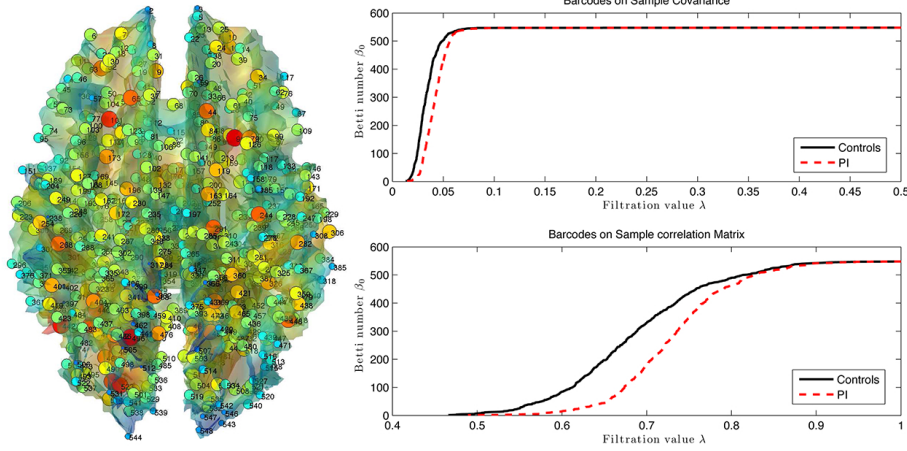


Fig. 5: Jacobian determinant of deformation field are measured at 548 nodes along the white matter boundary (Chung et al. 2015). The β_0 -number (number of connected components) of the filtrations on the sample correlations and covariances show huge group separation between normal controls and post-institutionalized (PI) children. The topological patterns are similar regardless of the number of nodes used.

and no two nodes between the different partitions are connected. The node and edge sets are denoted as $\mathcal{V}(\lambda) = \bigcup_{l=1}^{\kappa} V_l$ and $\mathcal{E}(\lambda) = \bigcup_{l=1}^{\kappa} E_l$ respectively. Then we have the following theorem:

Theorem 3. *The induced graph from the sparse correlation forms a filtration:*

$$\mathcal{G}(\lambda_1) \supset \mathcal{G}(\lambda_2) \supset \mathcal{G}(\lambda_3) \supset \dots \quad (18)$$

for $\lambda_1 \leq \lambda_2 \leq \lambda_3 \leq \dots$. Equivalently, the node and edge sets also form filtrations as well:

$$\begin{aligned} \mathcal{V}(\lambda_1) \supset \mathcal{V}(\lambda_2) \supset \mathcal{V}(\lambda_3) \supset \dots \\ \mathcal{E}(\lambda_1) \supset \mathcal{E}(\lambda_2) \supset \mathcal{E}(\lambda_3). \end{aligned}$$

The proof can be easily obtained from the definition of adjacency matrix (17).

3.3 Sparse cross-correlations

We can extend the sparse correlation framework to the sparse cross-correlations. Let $V = \{v_1, \dots, v_p\}$ be a node set where data is observed. We expect the number of nodes p to be significantly larger than the number of images n , i.e., $p \gg n$. Let $x_k(v_i)$ and $y_k(v_i)$ be the k -th paired scalar measurements at node v_i . They can be twins, longitudinal scans or even multimodal images. Denote

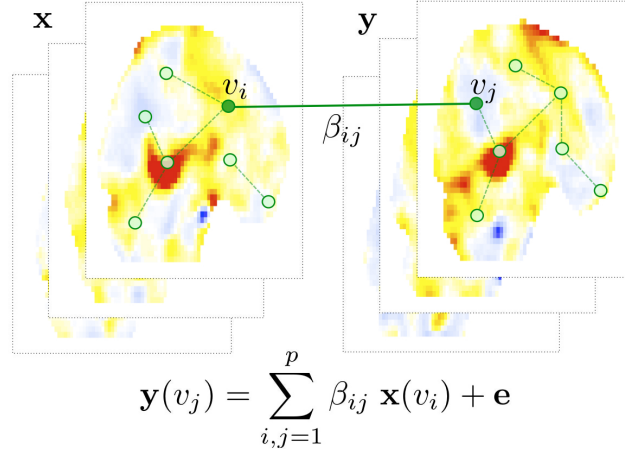


Fig. 6: The schematic of hyper-network construction on paired image vectors \mathbf{x} and \mathbf{y} . The image vectors \mathbf{y} at voxel v_j is modeled as a linear combination of the first image vector \mathbf{x} at all other voxels. The estimated parameters β_{ij} give the hyper-edge weights.

$\mathbf{x}(v_i) = (x_1(v_i), \dots, x_n(v_i))^\top$ and $\mathbf{y}(v_i) = (y_1(v_i), \dots, y_n(v_i))^\top$ be the paired data vectors over n different images at voxel v_i . Center and scale \mathbf{x} and \mathbf{y} such that

$$\sum_{k=1}^n x_k(v_i) = \sum_{k=1}^n y_k(v_i) = 0,$$

$$\|\mathbf{x}(v_i)\|^2 = \mathbf{x}^\top(v_i)\mathbf{x}(v_i) = \|\mathbf{y}(v_i)\|^2 = \mathbf{y}^\top(v_i)\mathbf{y}(v_i) = 1$$

for all v_i . The reasons for centering and scaling will soon be obvious.

We set up a hyper-network by relating the paired vectors at different voxels v_i and v_j :

$$\mathbf{y}(v_j) = \sum_{i=1}^p \beta_{ij} \mathbf{x}(v_i) + \mathbf{e} \quad (19)$$

for some zero-mean noise vector \mathbf{e} (Fig. 6). The parameters $\beta = (\beta_{ij})$ are the weights of the hyper-edges between voxels v_i and v_j that have to be estimated. We are constructing a physically nonexistent artificial network across different images. For fMRI, (19) requires estimating over billions of connections, which is computationally challenging. In practice however, each application will likely to force β to have a specific structure that may reduce the computational burden.

For this section, let us set up a linear model between $\mathbf{x}(v_i)$ and $\mathbf{y}(v_j)$:

$$\mathbf{y}(v_j) = b_{ij} \mathbf{x}(v_i) + \mathbf{e}, \quad (20)$$

where \mathbf{e} is the zero-mean error vector whose components are independent and identically distributed. Since the data are all centered, we do not have the intercept in linear regression (20). The least squares estimation (LSE) of b_{ij} that minimizes the L2-norm

$$\sum_{i,j=1}^p \|\mathbf{y}(v_j) - b_{ij} \mathbf{x}(v_i)\|^2 \quad (21)$$

is given by

$$\hat{b}_{ij} = \mathbf{x}^\top(v_i) \mathbf{y}(v_j), \quad (22)$$

which are the (sample) *cross-correlations* (Worsley, Charil, Lerch & Evans 2005, Worsley, Chen, Lerch & Evans 2005). The cross-correlation is invariant under the centering and scaling operations. The sparse version of L2-norm (21) is given by

$$F(\beta; \mathbf{x}, \mathbf{y}, \lambda) = \frac{1}{2} \sum_{i,j=1}^p \|\mathbf{y}(v_j) - \beta_{ij} \mathbf{x}(v_i)\|^2 + \lambda \sum_{i,j=1}^p |\beta_{ij}|. \quad (23)$$

The *sparse cross-correlation* is then obtained by minimizing over every possible $\beta_{ij} \in \mathbb{R}$:

$$\hat{\beta}(\lambda) = \arg \min_{\beta} F(\beta; \mathbf{x}, \mathbf{y}, \lambda). \quad (24)$$

The estimated sparse cross-correlations $\hat{\beta}(\lambda) = (\hat{\beta}_{ij}(\lambda))$ shrink toward zero as sparse parameter $\lambda \geq 0$ increases. The direct optimization of (23) for large p is computationally demanding. However, there is no need to optimize (23) numerically using the coordinate descent learning or the active-set algorithm as often done in sparse optimization (Peng et al. 2009, Friedman et al. 2008). We can show that the minimization of (23) is simply done algebraically.

Theorem 4. For $\lambda \geq 0$, the minimizer of $F(\beta; \mathbf{x}, \mathbf{y}, \lambda)$ is given by

$$\hat{\beta}_{ij}(\lambda) = \begin{cases} \mathbf{x}^\top(v_i) \mathbf{y}(v_j) - \lambda & \text{if } \mathbf{x}^\top(v_i) \mathbf{y}(v_j) > \lambda \\ 0 & \text{if } |\mathbf{x}^\top(v_i) \mathbf{y}(v_j)| \leq \lambda \\ \mathbf{x}^\top(v_i) \mathbf{y}(v_j) + \lambda & \text{if } \mathbf{x}^\top(v_i) \mathbf{y}(v_j) < -\lambda \end{cases}. \quad (25)$$

Although it is not obvious, Theorem 4 is related to the orthogonal design in LASSO (Tibshirani 1996) and the soft-shrinkage in wavelets (Donoho et al. 1995). To see this, let us transform linear equations (20) into a index-free matrix equation:

$$\begin{bmatrix} \mathbf{y}(v_1) & \cdots & \mathbf{y}(v_1) \\ \mathbf{y}(v_2) & \cdots & \mathbf{y}(v_2) \\ \vdots & \ddots & \vdots \\ \mathbf{y}(v_p) & \cdots & \mathbf{y}(v_p) \end{bmatrix} = \begin{bmatrix} b_{11} \mathbf{x}(v_1) & b_{21} \mathbf{x}(v_2) & \cdots & b_{p1} \mathbf{x}(v_p) \\ b_{12} \mathbf{x}(v_1) & b_{22} \mathbf{x}(v_2) & \cdots & b_{p2} \mathbf{x}(v_p) \\ \vdots & \vdots & \ddots & \vdots \\ b_{1p} \mathbf{x}(v_1) & b_{2p} \mathbf{x}(v_2) & \cdots & b_{pp} \mathbf{x}(v_p) \end{bmatrix} + \begin{bmatrix} \mathbf{e} & \cdots & \mathbf{e} \\ \mathbf{e} & \cdots & \mathbf{e} \\ \vdots & \ddots & \vdots \\ \mathbf{e} & \cdots & \mathbf{e} \end{bmatrix}.$$

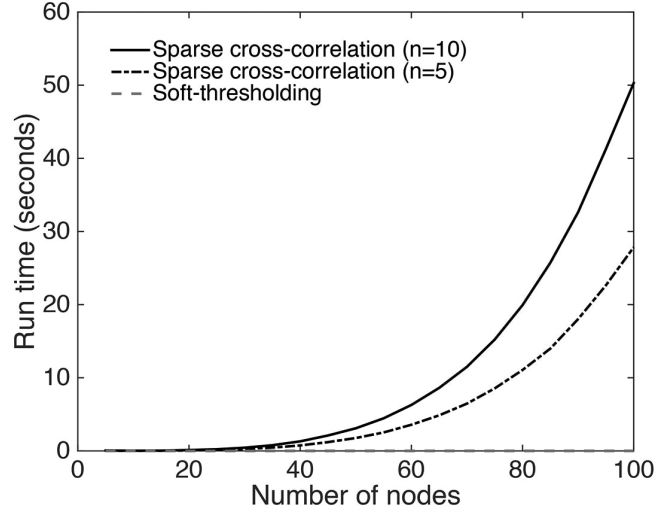


Fig. 8: Run time comparison of estimating sparse cross-correlations. The LASSO-based numerical optimization with $n = 5, 10$ images with varying number of nodes. The run time scale linearly with the number of images but scale exponentially with the number of nodes. The LASSO runs more than 100000 times slower compared to the soft-thresholding method for $p = 100$ nodes and $n = 10$ images.

where vec is the vectorization operation. The block diagonal design matrix \mathbb{X} consists of p diagonal blocks $I_p \otimes \mathbf{x}(v_1), \dots, I_p \otimes \mathbf{x}(v_p)$, where I_p is $p \times p$ identity matrix. Subsequently, $\mathbb{X}^\top \mathbb{X}$ is again a block diagonal matrix, where the i -th block is

$$[I_p \otimes \mathbf{x}(v_i)]^\top [I_p \otimes \mathbf{x}(v_i)] = I_p \otimes [\mathbf{x}(v_i)^\top \mathbf{x}(v_i)] = I_p.$$

Thus, \mathbb{X} is an orthogonal design. However, our formulation is *not* exactly the orthogonal design of LASSO as specified in (Tibshirani 1996) since the noise components in (26) are not independent. Further in standard LASSO, there are more columns than rows in \mathbb{X} . In our case, there are n times more rows. Still the soft-thresholding method introduced in (Tibshirani 1996) is applicable and we obtain the analytic solution, which speed up the computation drastically compared to existing LASSO-based numerical optimization (Figure 8) (Peng et al. 2009, Friedman et al. 2008).

Theorem 4 generalizes the sparse correlation case given in Chung et al. (2013). Figure 7-top displays an example of obtaining sparse cross-correlations from the initial sample cross-correlation matrix

$$\mathbf{X}^\top \mathbf{Y} = \begin{pmatrix} \times & 0.4 & 0.5 & -0.7 \\ \times & \times & 0.3 & -0.1 \\ \times & \times & \times & 0.9 \end{pmatrix}$$

using Theorem 4. Due to directional nature of the cross-correlation matrix, only the upper triangle part of the sample cross-correlation is demonstrated.

4 Partial correlation network

Let p be the number of nodes in the network. In most applications, the number of nodes is expected to be larger than the number of observations n , which gives an underdetermined system. Consider measurement vector at the j -th node

$$\mathbf{x}_j = (x_{1j}, \dots, x_{nj})^\top$$

consisting of n measurements. Vector \mathbf{x}_j are assumed to be distributed with mean zero and covariance $\Sigma = (\sigma_{ij})$. The correlation γ_{ij} between the two nodes i and j is given by

$$\gamma_{ij} = \frac{\sigma_{ij}}{\sqrt{\sigma_{ii}\sigma_{jj}}}.$$

By thresholding the correlation, we can establish a link between two nodes. However, there is a problem with this simplistic approach in that it fails to explicitly factor out the confounding effect of other nodes. To remedy this problem, partial correlations can be used in factoring out the dependency of other nodes (He et al. 2007, Marrelec et al. 2006, Huang et al. 2009, 2010, Peng et al. 2009).

If we denote the inverse covariance matrix as $\Sigma^{-1} = (\sigma^{ij})$, the *partial correlation* between the nodes i and j while factoring out the effect of all other nodes is given by (Peng et al. 2009)

$$\rho_{ij} = -\frac{\sigma^{ij}}{\sqrt{\sigma^{ii}\sigma^{jj}}}. \quad (27)$$

Equivalently, we can compute the partial correlation *via* a linear model as follows. Consider a linear model of correlating measurement at node j to all other nodes:

$$\mathbf{x}_j = \sum_{k \neq j} \beta_{jk} \mathbf{x}_k + \epsilon_k. \quad (28)$$

The parameters β_{jk} are estimated by minimizing the sum of squared residual of (28)

$$L(\beta) = \sum_{j=1}^p \|\mathbf{x}_j - \sum_{k \neq j} \beta_{jk} \mathbf{x}_k\|^2 \quad (29)$$

in a least squares fashion. If we denote the least squares estimator by $\widehat{\beta}_{jk}$, the residuals are given by

$$\mathbf{r}_j = \mathbf{x}_j - \sum_{k \neq j} \widehat{\beta}_{jk} \mathbf{x}_k. \quad (30)$$

The partial correlation is then obtained by computing the correlation between the residuals (He et al. 2007, Lerch et al. 2006, Peng et al. 2009):

$$\rho_{ij} = \text{corr}(\mathbf{r}_i, \mathbf{r}_j).$$

4.1 Sparse partial correlations

There is a serious problem with the least squares estimation framework discussed in the previous section. Since $n \ll p$, this is a significantly underdetermined system. This is also related to the covariance matrix Σ being singular so we cannot just invert the covariance matrix. For this, we need sparse network modeling.

The minimization of (29) is exactly given by solving the normal equation:

$$\mathbf{x}_j = \sum_{k \neq j} \beta_{jk} \mathbf{x}_k, \quad (31)$$

which can be turned into standard linear form $y = A\beta$ (Lee, Lee, Kang, Kim & Chung 2011). Note that (31) can be written as

$$\mathbf{x}_j = \underbrace{[\mathbf{x}_1, \dots, \mathbf{x}_{j-1}, \mathbf{0}, \mathbf{x}_{j+1}, \dots, \mathbf{x}_p]}_{\mathbf{X}_{-j}} \underbrace{\begin{pmatrix} \beta_{j1} \\ \beta_{j2} \\ \vdots \\ \beta_{jp} \end{pmatrix}}_{\beta_j},$$

where $\mathbf{0}_{n \times 1}$ is a column vector of all zero entries. Then we have

$$\underbrace{\begin{pmatrix} \mathbf{x}_1 \\ \mathbf{x}_2 \\ \vdots \\ \mathbf{x}_p \end{pmatrix}}_{y_{n \times p \times 1}} = \underbrace{\begin{pmatrix} \mathbf{X}_{-1} & \mathbf{0} & \cdots & \mathbf{0} \\ \mathbf{0} & \mathbf{X}_{-2} & \cdots & \mathbf{0} \\ \vdots & \vdots & \ddots & \vdots \\ \mathbf{0} & \mathbf{0} & \cdots & \mathbf{X}_{-p} \end{pmatrix}}_{A_{n \times p \times p^2}} \underbrace{\begin{pmatrix} \beta_1 \\ \beta_2 \\ \vdots \\ \beta_p \end{pmatrix}}_{\beta_{p^2 \times 1}}, \quad (32)$$

where A is a block diagonal matrix and $\mathbf{0}_{n \times p}$ is a matrix of all zero entries. We regularize (32) by incorporating l_1 LASSO-penalty J (Tibshirani 1996, Peng et al. 2009, Lee, Lee, Kang, Kim & Chung 2011):

$$J = \sum_{i,j} |\beta_{ij}|.$$

The sparse estimation of β_{ij} is then given by minimizing $L + \lambda J$. Since there is dependency between y and A , (32) is not exactly a standard compressed sensing problem (Peng et al. 2009, Lee, Lee, Kang, Kim & Chung 2011). It should be intuitively understood that sparsity makes the linear equation (31) less underdetermined. The larger the value of λ , the more sparse the underlying topological structure gets. Since

$$\rho_{ij} = \beta_{ij} \sqrt{\frac{\sigma^{ii}}{\sigma^{jj}}},$$

the sparsity of β_{ij} directly corresponds to the sparsity of ρ_{ij} , which is the strength of the link between nodes i and j (Peng et al. 2009, Lee, Lee, Kang, Kim & Chung 2011). Once the sparse partial correlation matrix ρ is obtained, we can simply link nodes i and j , if $\rho_{ij} > 0$ and assign the weight ρ_{ij} to the edge. This way, we obtain the weighted graph.

4.2 Limitations

However, the sparse partial correlation framework has a serious computational bottleneck. For n measurements over p nodes, it is required that we solve a linear system with an extremely large A matrix of size $np \times p^2$, so that the complexity of the problem increases by a factor of p^3 ! Consequently, for a large number of nodes, the problem immediately becomes almost intractable for a small computer. For example, for 1 million nodes, we have to compute 1 trillion possible pairwise relationships between nodes. One practical solution is to modify (28) so that the measurement at node i is represented more sparsely over some possible index set S_i :

$$x_i = \sum_{S_i} \beta_{ij} x_j + \epsilon_i.$$

making the problem substantially smaller.

An alternate approach is to simply follow the *homotopy path*, which adds network edges one by one with a very limited increase of computational complexity so there is no need to compute β repeatedly from scratch (Donoho & Tsaig 2006, Plumbley 2005, Osborne et al. 2000). The trajectory of the optimal solution β in LASSO follows a piecewise linear path as we change λ . By tracing the linear path, we can substantially reduce the computational burden of reestimating β when λ changes.

Acknowledgements

The part of this study was supported by NIH grants NIH R01 EB022856 and R01 EB028753. We would like to thank Anqi Qiu of National University of Singapore for providing the data used in Figure 1 and 2, and Seth Pollak of University of Wisconsin-Madison for the data used in Figure 5.

Bibliography

- Anderson, T. (1984), *An Introduction to Multivariate Statistical Analysis*, 2nd edn, Wiley.
- Avants, B., Cook, P., Ungar, L., Gee, J. & Grossman, M. (2010), ‘Dementia induces correlated reductions in white matter integrity and cortical thickness: a multivariate neuroimaging study with sparse canonical correlation analysis’, *NeuroImage* **50**, 1004–1016.
- Banerjee, O., El Ghaoui, L. & d’Aspremont, A. (2008), ‘Model selection through sparse maximum likelihood estimation for multivariate Gaussian or binary data’, *The Journal of Machine Learning Research* **9**, 485–516.
- Banerjee, O., Ghaoui, L., d’Aspremont, A. & Natsoulis, G. (2006), Convex optimization techniques for fitting sparse Gaussian graphical models, in ‘Proceedings of the 23rd International Conference on Machine Learning’, p. 96.
- Bickel, P. & Levina, E. (2008), ‘Regularized estimation of large covariance matrices’, *The Annals of Statistics* **36**, 199–227.
- Cao, J. & Worsley, K. (1999), ‘The detection of local shape changes via the geometry of Hotelling’s T2 fields’, *Annals of Statistics* **27**, 925–942.
- Chung, M., Hanson, J., Lee, H., Adluru, N., Alexander, A. L., Davidson, R. & Pollak, S. (2013), ‘Persistent homological sparse network approach to detecting white matter abnormality in maltreated children: MRI and DTI multimodal study’, *MICCAI, Lecture Notes in Computer Science (LNCS)* **8149**, 300–307.
- Chung, M., Hanson, J., Ye, J., Davidson, R. & Pollak, S. (2015), ‘Persistent homology in sparse regression and its application to brain morphometry’, *IEEE Transactions on Medical Imaging* **34**, 1928–1939.
- Chung, M., Vilalta-Gil, V., Lee, H., Rathouz, P., Lahey, B. & Zald, D. (2017), ‘Exact topological inference for paired brain networks via persistent homology’, *Information Processing in Medical Imaging (IPMI), Lecture Notes in Computer Science (LNCS)* **10265**, 299–310.
- Chung, M., Worsley, K., Brendon, M., Dalton, K. & Davidson, R. (2010), ‘General multivariate linear modeling of surface shapes using SurfStat’, *NeuroImage* **53**, 491–505.
- Chung, M., Worsley, K., Paus, T., Cherif, D., Collins, C., Giedd, J., Rapoport, J. & Evans, A. (2001), ‘A unified statistical approach to deformation-based morphometry’, *NeuroImage* **14**, 595–606.
- Donoho, D., Johnstone, I., Kerkycharian, G. & Picard, D. (1995), ‘Wavelet shrinkage: asymptopia?’, *Journal of the Royal Statistical Society. Series B (Methodological)* **57**, 301–369.
- Donoho, D. & Tsai, Y. (2006), *Fast solution of l_1 -norm minimization problems when the solution may be sparse*, Citeseer.
- Edelsbrunner, H. & Harer, J. (2008), ‘Persistent homology - a survey’, *Contemporary Mathematics* **453**, 257–282.

- Fornito, A., Zalesky, A. & Bullmore, E. (2010), ‘Network scaling effects in graph analytic studies of human resting-state fMRI data’, *Frontiers in Systems Neuroscience* **4**, 1–16.
- Friedman, J., Hastie, T. & Tibshirani, R. (2008), ‘Sparse inverse covariance estimation with the graphical lasso.’, *Biostatistics* **9**, 432.
- Friston, K., Holmes, A., Worsley, K., Poline, J.-P., Frith, C. & Frackowiak, R. (1995), ‘Statistical parametric maps in functional imaging: A general linear approach’, *Human Brain Mapping* **2**, 189–210.
- Gaser, C., Volz, H.-P., Kiebel, S., Riehemann, S. & Sauer, H. (1999), ‘Detecting structural changes in whole brain based on nonlinear deformations - Application to schizophrenia research’, *NeuroImage* **10**, 107–113.
- Gong, G., He, Y., Concha, L., Lebel, C., Gross, D., Evans, A. & Beaulieu, C. (2009), ‘Mapping anatomical connectivity patterns of human cerebral cortex using in vivo diffusion tensor imaging tractography’, *Cerebral Cortex* **19**, 524–536.
- Hagmann, P., Kurant, M., Gigandet, X., Thiran, P., Wedeen, V., Meuli, R. & Thiran, J. (2007), ‘Mapping human whole-brain structural networks with diffusion MRI’, *PLoS One* **2**(7), e597.
- He, Y., Chen, Z. & Evans, A. (2007), ‘Small-world anatomical networks in the human brain revealed by cortical thickness from MRI’, *Cerebral Cortex* **17**, 2407–2419.
- He, Y., Chen, Z. & Evans, A. (2008), ‘Structural insights into aberrant topological patterns of large-scale cortical networks in Alzheimer’s disease’, *Journal of Neuroscience* **28**, 4756.
- Hsieh, C.-J., Sustik, M., Dhillon, I., Ravikumar, P. & Poldrack, R. (2013), BIG & QUIC: Sparse inverse covariance estimation for a million variables, in ‘Advances in Neural Information Processing Systems’, pp. 3165–3173.
- Huang, S., Li, J., Sun, L., Liu, J., Wu, T., Chen, K., Fleisher, A., Reiman, E. & Ye, J. (2009), Learning brain connectivity of Alzheimer’s disease from neuroimaging data, in ‘Advances in Neural Information Processing Systems’, pp. 808–816.
- Huang, S., Li, J., Sun, L., Ye, J., Fleisher, A., Wu, T., Chen, K. & Reiman, E. (2010), ‘Learning brain connectivity of Alzheimer’s disease by sparse inverse covariance estimation’, *NeuroImage* **50**, 935–949.
- Joshi, S. (1998), Large Deformation Diffeomorphisms and Gaussian Random Fields for Statistical Characterization of Brain Sub-Manifolds, PhD thesis, Washington University, St. Louis.
- Lee, H., Chung, M., Kang, H., Kim, B.-N. & Lee, D. (2011), ‘Computing the shape of brain networks using graph filtration and Gromov-Hausdorff metric’, *MICCAI, Lecture Notes in Computer Science* **6892**, 302–309.
- Lee, H., Kang, H., Chung, M., Kim, B.-N. & Lee, D. (2012), ‘Persistent brain network homology from the perspective of dendrogram’, *IEEE Transactions on Medical Imaging* **31**, 2267–2277.
- Lee, H., Lee, D., Kang, H., Kim, B.-N. & Chung, M. (2011), ‘Sparse brain network recovery under compressed sensing’, *IEEE Transactions on Medical Imaging* **30**, 1154–1165.

- Lerch, J., Worsley, K., Shaw, W., Greenstein, D., Lenroot, R., Giedd, J. & Evans, A. (2006), ‘Mapping anatomical correlations across cerebral cortex (MACACC) using cortical thickness from MRI’, *NeuroImage* **31**, 993–1003.
- Marrelec, G., Krainik, A., Duffau, H., Péligrini-Issac, M., Lehericy, S., Doyon, J. & Benali, H. (2006), ‘Partial correlation for functional brain interactivity investigation in functional MRI’, *NeuroImage* **32**, 228–237.
- Mazumder, R. & Hastie, T. (2012), ‘Exact covariance thresholding into connected components for large-scale graphical LASSO’, *The Journal of Machine Learning Research* **13**, 781–794.
- Osborne, M., Presnell, B. & Turlach, B. (2000), ‘A new approach to variable selection in least squares problems’, *IMA Journal of Numerical Analysis* **20**, 389–404.
- Peng, J., Wang, P., Zhou, N. & Zhu, J. (2009), ‘Partial correlation estimation by joint sparse regression models’, *Journal of the American Statistical Association* **104**, 735–746.
- Plumbley, M. (2005), ‘Geometry and homotopy for l_1 sparse representations’, *Proceedings of SPARS* **5**, 206–213.
- Qiu, A., Lee, A., Tan, M. & Chung, M. (2015), ‘Manifold learning on brain functional networks in aging’, *Medical image analysis* **20**, 52–60.
- Schäfer, J. & Strimmer, K. (2005), ‘A shrinkage approach to large-scale covariance matrix estimation and implications for functional genomics’, *Statistical Applications in Genetics and Molecular Biology* **4**, 32.
- Taylor, J. & Worsley, K. (2008), ‘Random fields of multivariate test statistics, with applications to shape analysis’, *Annals of Statistics* **36**, 1–27.
- Thompson, P., MacDonald, D., Mega, M., Holmes, C., Evans, A. & Toga, A. (1997), ‘Detection and mapping of abnormal brain structure with a probabilistic atlas of cortical surfaces’, *Journal of Computer Assisted Tomography* **21**, 567–581.
- Tibshirani, R. (1996), ‘Regression shrinkage and selection via the LASSO’, *Journal of the Royal Statistical Society. Series B (Methodological)* **58**, 267–288.
- Witten, D., Friedman, J. & Simon, N. (2011), ‘New insights and faster computations for the graphical LASSO’, *Journal of Computational and Graphical Statistics* **20**, 892–900.
- Worsley, K., Charil, A., Lerch, J. & Evans, A. (2005), Connectivity of anatomical and functional MRI data, in ‘Proceedings of IEEE International Joint Conference on Neural Networks (IJCNN)’, Vol. 3, pp. 1534–1541.
- Worsley, K., Chen, J., Lerch, J. & Evans, A. (2005), ‘Comparing functional connectivity via thresholding correlations and singular value decomposition’, *Philosophical Transactions of the Royal Society B: Biological Sciences* **360**, 913.
- Worsley, K., Marrett, S., Neelin, P., Vandal, A., Friston, K. & Evans, A. (1996), ‘A unified statistical approach for determining significant signals in images of cerebral activation’, *Human Brain Mapping* **4**, 58–73.
- Worsley, K., Taylor, J., Tomaiuolo, F. & Lerch, J. (2004), ‘Unified univariate and multivariate random field theory’, *NeuroImage* **23**, S189–195.

- Xin, B., Hu, L., Wang, Y. & Gao, W. (2015), Stable feature selection from brain sMRI, *in* 'Proceedings of the Twenty-Ninth AAAI Conference on Artificial Intelligence', pp. 1910–1916.
- Zalesky, A., Fornito, A., Harding, I., Cocchi, L., Yücel, M., Pantelis, C. & Bullmore, E. (2010), 'Whole-brain anatomical networks: Does the choice of nodes matter?', *NeuroImage* **50**, 970–983.